

Fast singular value decomposition combined maximum entropy method for plasma tomography

Junghee Kim and W. Choe^{a)}

Department of Physics, Korea Advanced Institute of Science and Technology, 373-1 Guseong-dong, Yuseong-gu, Daejeon 305-701, Korea

(Received 5 October 2005; accepted 4 December 2005; published online 24 February 2006)

The maximum entropy method (MEM) is a widely used reconstruction algorithm in plasma physics. Drawbacks of the conventional MEM are its heavy time-consuming process and possible generation of noisy reconstruction results. In this article, a modified maximum entropy algorithm is described which speeds up the calculation and shows better noise handling capability. Similar to the rapid minimum Fisher information method, the modified maximum entropy algorithm uses simple matrix operations instead of treating a fully nonlinear problem. The preprocess for rapid tomographic calculation is based on the vector operations and the singular value decomposition (SVD). The initial guess of the sought-for emissivity is calculated by SVD and this helped reconstruction about ten times faster than the conventional MEM. Therefore, the developed fast MEM can be used for intershot tomographic analyses of fusion plasmas. © 2006 American Institute of Physics.

[DOI: [10.1063/1.2169489](https://doi.org/10.1063/1.2169489)]

I. INTRODUCTION

Maximum entropy method (MEM) is a widely used powerful tomographic technique for reconstruction and restoration of images used in various application areas. For example, it has been used in astronomy as an image processing tool for extracting interested astronomical objects and deblurring¹⁻³ of images. In fusion plasma research, the inner structure of plasma can be reconstructed by MEM using a well-made weight matrix. However, there exists a possibility of errors in the reconstructed image with respect to the real image because of the ill-posedness of the tomography problem caused by the nonuniformly distributed detectors around the plasma due to the geometrical accessibility limitation of fusion devices. Robust tomography algorithms are needed to achieve reliable reconstruction results, and a few widely used examples include MEM, minimum Fisher information method, and Tikhonov-type regularizations. In order to minimize the characteristic functional consisting of χ^2 and the information entropy S in these algorithms, the least squared solution has to be achieved and S should be maximized. This solution is the most feasible result of the highly underdetermined problem (for instance, with 192 equations or measurements and 3500 variables or pixels). The ill-posedness of the tomography problem increases as the number of pixels is increased, and the tomographic solution becomes more unstable and noisy as the ill-posedness becomes larger.

In this article, a modified maximum entropy method is reported with which calculation speed and noise handling capability of the conventional maximum entropy algorithm is significantly improved. In our modified MEM, vector operation is adopted instead of using matrix inversion, and the

uncorrelation between adjacent pixels in the framework of MEM is overcome with the help of singular value decomposition (SVD). We introduce the modification of the conventional MEM in Sec. II. The reconstruction test results are described in Sec. III, and it is followed by discussions and conclusions in Sec. IV.

II. FAST MAXIMUM ENTROPY METHOD

A. Maximum entropy algorithm

The maximum entropy algorithm selects a solution that maximizes the information entropy of the emissivity distribution. With a two-dimensional image regarded as a set of pixels with positive numbers g_1, g_2, \dots, g_N where N is the number of pixels, the entropy S can be defined in information-theoretic terms⁴ as

$$S = - \sum_{j=1}^N p_j \log p_j,$$

$$p_j = g_j / \sum_{j=1}^N g_j. \quad (1)$$

If the intensity pattern $g_j(j=1, \dots, N)$ of an image is given, the entropy S indicates the number of bits of information needed to localize the position of the j th pixel of a single radiated photon. The conventional maximum entropy method deals with a nonlinear constrained optimization problem in finding the solution that maximizes S . The main drawback of the conventional MEM is that it is time consuming due mainly to the matrix inversion. However, the calculation time can be significantly reduced by adopting the singular value decomposition and vector operations instead of the matrix inversion. Before the modified algorithm is discussed

^{a)} Author to whom correspondence should be addressed; electronic mail: wchoe@kaist.ac.kr

in detail, a brief description about the maximum entropy algorithm is given.

With M detectors and N pixels, the measured line-integrated data, represented as a column vector \mathbf{f} ($M \times 1$ matrix), are related to the desired local pixel data, represented as a column vector \mathbf{g} ($N \times 1$ matrix), and the weight matrix \underline{W}

$$f_k = D_k + \varepsilon_k, \quad (2)$$

$$D_k = \sum_{j=1}^N W_{kj} g_j \quad (k = 1, \dots, M).$$

The weight matrix \underline{W} describes the geometrical layout of the detectors and its element W_{kj} indicates the contribution of the j th pixel to the k th detector. ε_k in Eq. (2) denotes the standard error due to the random noise in the k th detector measurement with zero mean. Because of the existence of the error ε_k , the direct inversion of the weight matrix is not a proper way to seek a reliable solution \mathbf{g} . Therefore, regularization methods such as MEM have usually been adopted to solve the highly ill-posed problem of the linear equation set where the number of pixels is much larger than that of detectors in the presence of an accompanying noise. To avoid the ill-posedness and to obtain a unique solution, we solve the problem using the Bayesian probability theory (BPT). The posterior probability density function based on the BPT is written as³

$$p(\mathbf{g}|\mathbf{f}, \sigma, I) = \frac{p_p(\mathbf{g}|I) \cdot p_l(\mathbf{f}|\mathbf{g}, \sigma, I)}{p_e(\mathbf{f}|I)}, \quad (3)$$

where $p_p(\mathbf{g}|I)$ is a prior probability density function, $p_l(\mathbf{f}|\mathbf{g}, \sigma, I)$ is a likelihood probability density function, $p_e(\mathbf{f}|I)$ is a normalization factor of the posterior probability density function, and I is the background expert knowledge. In tomography problems, the likelihood probability density function $p_l(\mathbf{f}|\mathbf{g}, \sigma, I)$ follows the error statistics of the experimental data. If the mean of a Gaussian error $\langle \varepsilon \rangle$ is zero and the standard deviation is σ , p_l is usually represented in terms of χ^2 statistics as

$$p_l(\mathbf{f}|\mathbf{g}, \sigma, I) = \frac{1}{M \prod_{k=1}^M \sqrt{2\pi}\sigma_k} \exp\left(-\frac{1}{2}\chi^2\right), \quad (4)$$

$$\chi^2 = \sum_{k=1}^M \left(\frac{f_k - \sum_{i=1}^N W_{ki} g_i}{\sigma_k} \right)^2, \quad (5)$$

where M and N are the number of detectors and pixels, respectively. The expert knowledge of the maximum entropy concept is that the image intensity of each pixel is greater than zero, and it is automatically included in the prior information $p_p(\mathbf{g}|I)$ by the entropic prior as follows:

$$p_p(\mathbf{g}|I) = \left(\frac{\alpha}{2\pi} \right)^{N/2} \exp(\alpha S). \quad (6)$$

Here, the regularization coefficient α is a competition factor between the entropy S of the image data and the χ^2 of the measured data \mathbf{f} . The condition which maximizes the poste-

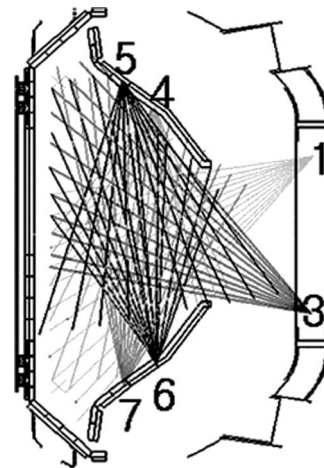


FIG. 1. The optimized layout of the KSTAR soft x-ray arrays (see Ref. 9) in which six arrays and 32 detector channels per array are considered. Tomographic reconstruction tests were performed based on the setup.

rior probability density function p in Eq. (3) leads to the fact that the global maximum of the following Eq. (7) exists

$$\Lambda(g, f) = \alpha S - \frac{1}{2}\chi^2. \quad (7)$$

Because the entropy S is a convex function and χ^2 is a convex ellipsoidal in a N -dimensional image space, there exists a unique solution for Eq. (7) which has the maximum entropy and the adaptive χ^2 . When the maximum entropy solution \mathbf{g} is obtained from Eqs. (3)–(6) by using methods such as the Lagrange multiplier method, the condition for which a unique solution for Eq. (7) exists establishes the following equation:

$$\alpha \frac{\partial S}{\partial g} - \frac{1}{2} \frac{\partial \chi^2}{\partial g} = 0 \quad (g = \hat{g}). \quad (8)$$

However, the maximum entropy algorithm may produce noisy reconstruction results compared with other kinds of reconstruction algorithms due to no correlation among adjacent pixels, and the results may bring about wrong interpretations. For instance, since the soft x-ray emissivity in tokamak plasmas is usually strongly correlated with the magnetic field configuration, the “noisy” result can be regarded as unexpected unreal magnetic islands or fluctuations. Moreover, the calculation speed of the conventional MEM is relatively low. Therefore, the conventional MEM may not be appropriate for intershot analyses of tokamak plasmas.

B. Modified algorithm

The MEM discussed here uses vector operations¹ rather than the matrix inversion. As a result, a very fast calculation can be achieved compared to the conventional MEM described in the previous subsection. Moreover, the image-data transformation by the weight matrix is carried out by transposing the weight matrix instead of using a pseudoinverse of the weight matrix. This type of MEM can be used for the analysis of multimega pixel astronomical images¹ and can also be applied to the superhigh resolution image analysis of fusion plasmas. Because usual tomographic analyses for Korea Superconducting Tokamak Advanced Research (KSTAR) plasmas (see Fig. 1) is planned to require an image that con-

sists of only 3500 pixels, tomographic results can be obtained in a relatively short time. Usually, the major computational load lies in the image-data transformations, and these can be coded efficiently using built-in mathematical packages.

Because the entropy S is a nonlinear logarithmic function of the image data as expressed in Eq. (1), a computational problem of finding the local information g becomes a kind of nonlinear constrained optimization problem. When dealing with many-pixel image data, it is not possible to use methods such as Newton–Raphson iteration and the Lagrange-multiplier method because the computational load is very high. The computing time increases considerably when the problem includes nonlinear nature and repeated transformation of the precalculated weight matrix.

Before going into simple matrix operations, the derivative (gradient) of c^2 is calculated by applying the chain rule to Eq. (7) to determine how to adjust a trial image data to fit the experimentally obtained data:

$$\frac{\partial \chi^2}{\partial g_j} = \sum_{k=1}^M \left(\frac{\partial D_k}{\partial g_j} \right) \left(\frac{\partial \chi^2}{\partial D_k} \right) = \sum_{k=1}^M \frac{2W_{jk}(D_k - f_k)}{\sigma_k^2}, \quad (9)$$

$$\frac{\partial S}{\partial g_j} = \sum_{i=1}^N \frac{g_i \log g_i}{\sum_{i=1}^N g_i} - \log g_j, \quad (10)$$

$$\frac{\partial^2 S}{\partial g_i \partial g_j} = -\frac{\delta_{ij}}{g_j}.$$

In this modified MEM algorithm, the transpose of the weight matrix W^T [W_{jk} in Eq. (9)] is used instead of the inverse matrix W^{-1} to increase the calculation speed. In practice, Eq. (2) is ill conditioned, so the direct recovery of the desired local pixel data g in Eq. (2) from the measured data f by calculating W^{-1} will fail. It is apparent that the vector operation such as the scalar product instead of using matrix operations significantly raises the efficiency of the ME algorithm. In order to find a solution for Eq. (7), the search direction method⁵ which uses three directional vectors

$$\begin{aligned} \mathbf{v}_1 &= \nabla \Lambda \\ \mathbf{v}_2 &= (\nabla \nabla \Lambda) \cdot \nabla \Lambda, \\ \mathbf{v}_3 &= (\nabla \nabla \nabla \Lambda) \cdot \nabla \Lambda \end{aligned} \quad (11)$$

is used where Λ is already defined in Eq. (8). The regularization parameter α is obtained purely by the chi square.^{1,3}

Once S , c^2 , and $\alpha^{(n)}$ are found, the desired emissivity solution is obtained from the derivative of the functional Λ by the following iterative representation [Eq. (12)], which is similar to the Newton–Raphson iteration method^{1,6}

$$g_j^{(n+1)} = g_j^{(n)} \left(1 + \alpha^{(n)} \frac{\partial S}{\partial g_j} - \frac{1}{2} \frac{\partial \chi^2}{\partial g_j} \right). \quad (12)$$

Here, the regularizing coefficient $\alpha^{(n)}$ is calculated from the directional method.⁵ Equation (12) is calculated from Eqs. (9) and (10). Because the iteration in Eq. (12) does not include an equation solving the process such as the Lagrange-

multiplier method, iteration speed is usually dramatically increased. Moreover, a proper initial guess ($g_j^{(0)}$) decreases the number of iterations and thus, the calculation time is decreased.

C. Singular value decomposition

Although we use a robust fast algorithm, there is a horizontal (major-radial) asymmetry due to the detection geometry of the fusion devices, and there also exists an error on the reconstructed image because the image pixel data set is regarded as a random variable set when the reconstruction algorithm is based on the MEM. Moreover, there is a strong correlation between adjacent image pixels because a fusion plasma is confined by strong magnetic fields and soft x-ray emissivity distribution is closely connected to the magnetic field configuration. Therefore, adding some correlation to the maximum entropy algorithm is needed to avoid a noisy result caused by the randomness of the reconstructed pixel data. In order to achieve it, magnetic equilibrium data from the internal magnetic diagnostic coils are often used. In other words, the tomographic result is fitted to the magnetic geometry. However, in the case of high beta plasmas, the location of the emissivity peak is sometimes mismatched to the peak of the magnetic field contours in the core region.⁷ In this case, there is a possibility that the fitted emissivity to the magnetic field may not be reliable, and therefore, a purely unbiased reconstruction algorithm is required.

Here we investigated a partly biased fast ME algorithm for the reconstruction using only sample array data without using any other kinds of diagnostic data to avoid the randomness in the maximum entropy reconstructed image data. It was carried out by using the SVD. The initial guess of the conventional MEM is obtained from the flat model in which each pixel data is calculated from the global averaging scheme. The flat model cannot avoid the uncorrelation among the adjacent pixels. Therefore, we replaced the flat model with the directly inverted model, which is a simply inverted result by the inverted weight matrix using SVD. In particular, the truncated singular value decomposition (TSVD) was used for the rectangular matrix inversion to avoid unexpected islands on the reconstructed image.⁸ The direct inversion with the help of SVD is not appropriate for solving a highly ill-posed tomography problem. However, because this pseudoinverse solution shows a minimum norm of the image space, the converging speed of the maximum entropy algorithm is increased. There is one problem owing to the negativity of the initial guess ($g_j^{(0)}$) from the SVD inversion. The absolute value of the negative value of the initially guessed image is lower than the background of the sample image and it appears at the very low intensity region. Therefore, this negative value can be regarded as an ignorable background value in the image, and the minimum norm of the initially guessed image space is still guaranteed although the value of the SVD-inverted initial image is slightly changed. Moreover, from the fact that the modified MEM using the SVD-inverted model produces a large value of the maximum posterior probability compared with the case using

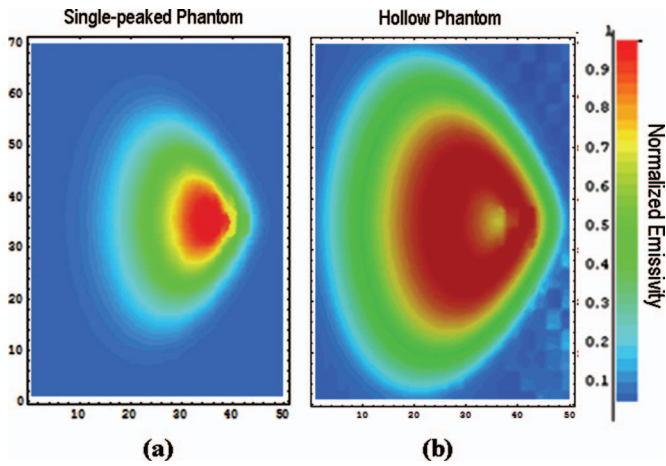


FIG. 2. (Color) The phantoms chosen for reconstruction tests: (a) single peaked profile and (b) hollow profile

the flat model, we can say that the modified MEM still follows the maximum entropy concept.

Another advantage of this modified MEM is that the maximum entropy solution converges after two or three iterations with high calculation speed. The SVD combined MEM guarantees a high accuracy on the overall region of the reconstructed image, and the test results are found in the following section.

III. RECONSTRUCTION TESTS

In this section, results of the tomographic reconstruction tests by the SVD combined MEM are described. The detector system considered for the tests is the one for KSTAR soft x-ray diagnostics, in which there are six detector arrays and a total of 192 detector channels.⁹ Each array has two V-shaped 16-channel detectors to increase the detection efficiency of the edge channels. The phantoms used for the reconstruction tests include random noise to simulate any noise associated with measurements. The relative noise was calculated based on the Gaussian probability distribution of 1% and 2% standard deviation with zero mean value.

The numerical code was developed using MATHEMATICA 5.0 high-level mathematical programming language. Because our modified MEM includes vector operations, list manipulations, and built-in linear algebraic packages, the MATHEMATICA-based code shows a powerful computing capability, fast coding, and easy optimization. All test calculations were performed on a Pentium IV 2.4 GHz processor under the Linux platform.

We chose two different kinds of emissivity phantom images expected in KSTAR plasmas as shown in Fig. 2: one is a single-peaked image sample and the other is a hollow-shaped sample. Each phantom consists of 70 (vertical) \times 50 (horizontal) pixels. The emission phantoms are based on the KSTAR-like magnetic flux surfaces of which the elon-

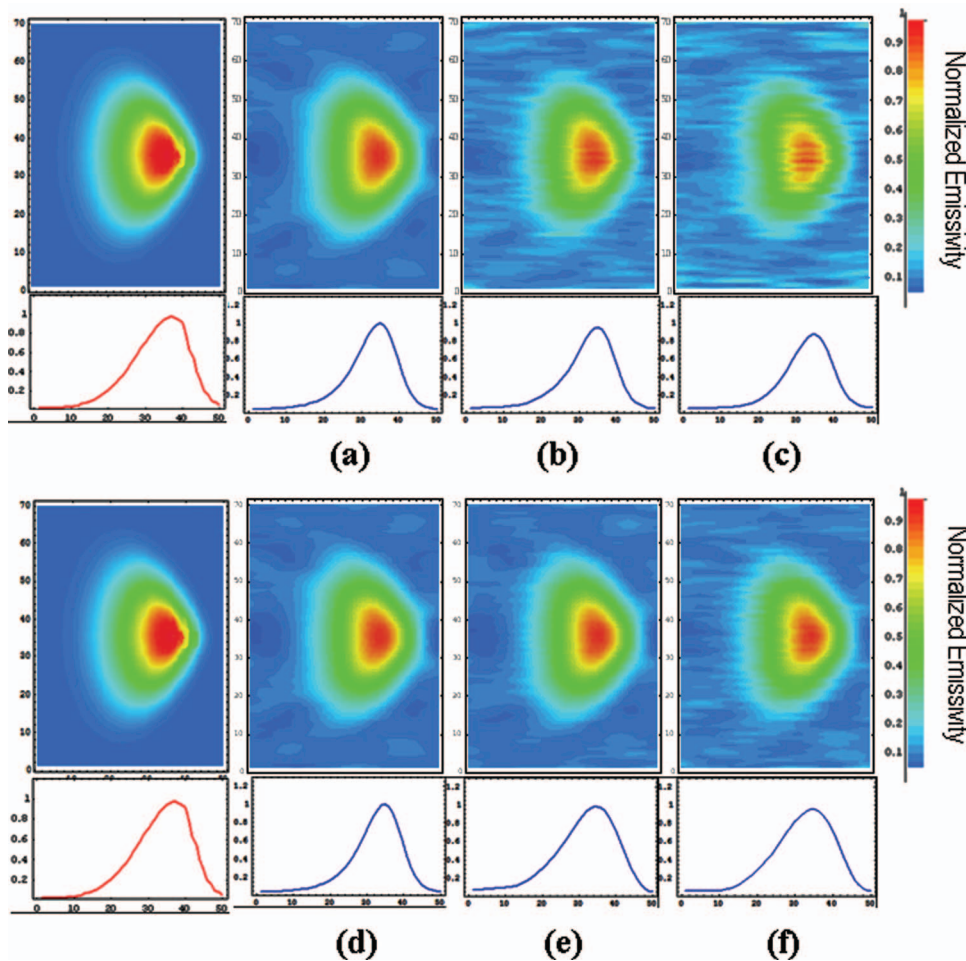


FIG. 3. (Color) Reconstruction results of the single-peaked phantom by the conventional MEM (a)–(c), and by the fast MEM (d)–(f). No noise was added in (a) and (d), 1% Gaussian noise was added in (b) and (e), and 2% Gaussian noise was added in (c) and (f). The bottom plots represent the emissivity profile along the midplane. The red curve shows that of the phantom.

TABLE I. Performance comparison (mean error and calculation time) between the conventional MEM and the modified fast MEM. Here, 0% indicates the case with no noise added. 1% and 2% represent the case with 1% and 2% Gaussian noises added to the simulated measurements, respectively.

Method	Profile	Mean error _{0%} (%)	Mean error _{1%} (%)	Mean error _{2%} (%)	Calculation time (s)
Conventional MEM	Single	6.90	8.20	8.70	20
	Hollow	5.72	6.85	8.83	
Modified fast MEM	Single	4.89	5.03	5.68	2
	Hollow	5.00	5.42	6.12	

gation κ is 1.8, the triangularity δ is 0.6, and the major and minor radius are 1.8 m and 0.5 m, respectively.¹⁰

Tomographic reconstructions were performed using line-integrated data evaluated from the given phantoms. A comparison between the single-peaked profiles depicted in Fig. 2(a) and Fig. 3 shows a pretty good result over the whole region of the image. Table I summarizes the mean error and the calculation time between the conventional MEM and our modified MEM, where the mean error by the modified MEM is overall smaller. It should also be noted that the calculation speed of the modified MEM is about ten times faster. The amount of the unreal background emissivity appeared outside the last closed flux surface by the conventional MEM

seems to be brighter (sky blue) than that by the fast MEM (9.52% mean error by the conventional MEM versus 7.10% by the modified fast MEM). The SVD-based initial guess of the reconstruction allows the adjacent pixels to link smoothly. This smoothing procedure enhances the spatial reliability of the entire reconstruction result for not only a single peaked pattern but also a hollow-shaped emissivity pattern.

As depicted in Fig. 4 where the hollow phantom [Fig. 2(b)] reconstructions are given, the modified MEM shows a pretty good reconstruction result both in the two-dimensional image and the emissivity profile along the midplane in contrast to the case of the conventional MEM. It is observed that the conventional MEM produces a significant noise when a 2% Gaussian noise was added to the simulated measurement. In contrast to the conventional MEM, the modified MEM shows good noise handling capability as shown in (d)–(f) of Figs. 3 and 4. In order to obtain the magnetohydrodynamics (MHD) mode structure from the reconstructed soft x-ray images,¹¹ it is important to achieve nondistorted reconstruction images. As demonstrated in Figs. 3 and 4, the modified fast maximum entropy algorithm may be very useful for handling noisy experimental data.

Quantitative comparisons were made in Table I with a mean reconstruction error σ defined as

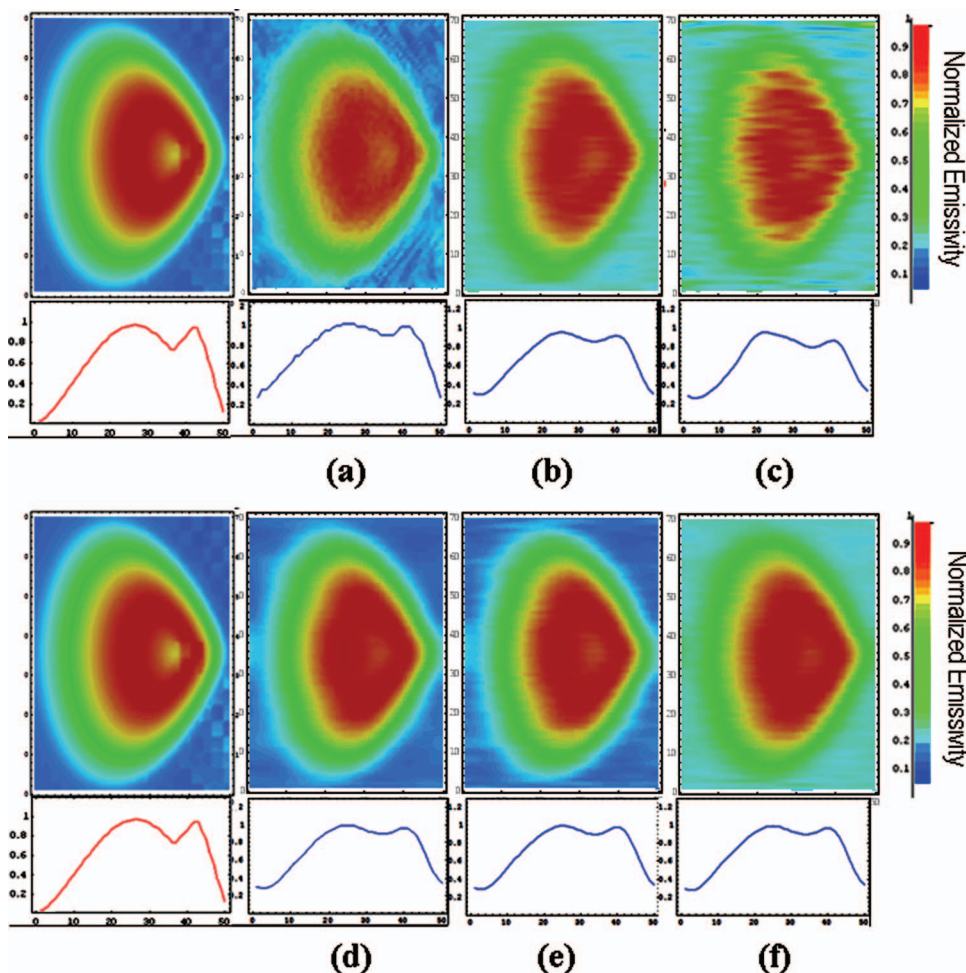


FIG. 4. (Color) Reconstruction results of the hollow-shaped phantom by the conventional MEM (a)–(c) and by the fast MEM (d)–(f). No noise was added in (a) and (d), 1% Gaussian noise was added in (b) and (e), and 2% Gaussian noise was added in (c) and (f). The bottom plots represent the emissivity profile along the midplane. The red curve shows that of the phantom.

$$\sigma = \sqrt{\langle (g_i^{\text{recon}} - g_i^{\text{phantom}})^2 \rangle}, \quad (13)$$

where $\langle \rangle$ denotes an average over all pixels, and g_i^{recon} and g_i^{phantom} are the i th pixel element of the reconstructed pixel image and the emissivity phantom, respectively. As shown in Table I, the numerical error tolerance of the modified MEM is superior to that of the conventional MEM by 1.2–1.5 times without loss of accuracy.

IV. DISCUSSION AND CONCLUSIONS

In this article, we investigated a modified fast MEM that improves calculation speed and random noise handling capability. The SVD used in the modified algorithm is a very helpful tool for reconstructing emission patterns. Because the SVD, which gives the minimum-norm nature of the solution set to the sought-for image solution, offers the geometrical considerations to the initial model of the inversion algorithm, the reconstructed profile becomes more reliable and less noisy. The most important character of the method is that the MEM can show very fast calculation speed without reducing accuracy. As a result, the modified fast MEM can effectively be utilized for intershot analyses of tokamak plasmas.

The work described in this article will be implemented with various regularizing inversion methods using linear algebraic techniques. This regularizing technique will also be useful for seeking solution of a highly ill-posed algebraic

equation set including a few nonlinear terms. Moreover, this SVD combined fast MEM can be applied to various kinds of emission tomography problems as well as soft x-ray tomography on arbitrarily shaped tokamak plasmas. The numerical code developed here will be implemented to a user-friendly graphical user interface by MATHEMATICA 5.2 and we expect that the real-time tomography will be possible with the help of the 64-bit computing environment.

ACKNOWLEDGMENT

This work was supported by the Ministry of Science and Technology of the Republic of Korea under the contract of KSTAR project.

- ¹J. Skilling and R. K. Bryan, *Mon. Not. R. Astron. Soc.* **211**, 111 (1984).
- ²J. Skilling, in *Maximum Entropy and Bayesian Methods*, edited by P. F. Fougere (Kluwer Academic, Norwell, MA, 1990).
- ³D. S. Sivia, *Bayesian Tutorial of Data Analysis* (Oxford University Press, Oxford, 1994).
- ⁴C. E. Shannon, *Bell Syst. Tech. J.* **27**, 379 (1948); **27**, 623 (1948).
- ⁵*Numerical Recipes in C* (Addison Wesley, Reading, MA, 1992).
- ⁶K. Ertl *et al.*, *Nucl. Fusion* **36**, 1477 (1996).
- ⁷J. Mlynar *et al.*, *Plasma Phys. Controlled Fusion* **45**, 169 (2003).
- ⁸P. Christian, *Rank-Deficient and Discrete Ill-Posed Problems: Numerical Aspects of Linear Inversion* (SIAM, Philadelphia, 1998).
- ⁹J. Kim and W. Choe, *Rev. Sci. Instrum.* **75**, 3974 (2004).
- ¹⁰G. S. Lee *et al.*, *Nucl. Fusion* **40**, 575 (2000).
- ¹¹M. Anton *et al.*, *Plasma Phys. Controlled Fusion* **38**, 1849 (1996).